

On quark-lepton mixing and the leptonic CP violation

Alessio Giarnetti^{*}, Simone Marciano[†], Davide Meloni[‡]

*Dipartimento di Matematica e Fisica, Università di Roma Tre
INFN Sezione di Roma Tre, Via della Vasca Navale 84, 00146, Roma, Italy*

Abstract

In the absence of a Grand Unified Theory framework, connecting the values of the mixing parameters in the quark and lepton sector is a difficult task, unless one introduces ad-hoc relations among the matrices that diagonalize such different kinds of fermions. In this paper, we discuss in detail the possibility that the PMNS matrix is given by the product $U_{PMNS} = V_{CKM}^* T^*$, where T comes from the diagonalization of a see-saw like mass matrix that can be of a Bimaximal (BM), Tri-Bimaximal (TBM) and Golden Ratio (GR) form, and identify the leading corrections to such patterns that allow a good fit to the leptonic mixing matrix as well as to the CP phase. We also show that the modified versions of BM, TBM and GR can easily accommodate the solar and atmospheric mass differences.

Contents

1	Introduction	1
2	Corrections to BM, TBM and GR	3
3	On the neutrino masses	13
4	Conclusions	16

1 Introduction

In the last years, neutrino experiments confirmed that neutrinos oscillate and measured with a great precision the values of the mixing angles. Some neutrino oscillation properties are still unknown/not really clear (as, for example, whether CP violation exists in the lepton sector or

^{*}e-mail address: alessio.giarnetti@uniroma3.it

[†]e-mail address: simone.marciano@uniroma3.it

[‡]e-mail address: davide.meloni@uniroma3.it

whether the mass hierarchy is of normal or inverted type) but the emerging picture is quite intriguing: differently from the mixing angles in the quark sector, described by an almost diagonal matrix V_{CKM} , neutrino mixing is dictated by two large and one small angle, thus making the U_{PMNS} a matrix with large entries, except for the (13) element. In spite of this huge discrepancy (that has been dubbed as *the flavor problem*), the current numerical values of fermion mixings seem to be inextricably wedged into well-defined relations [1] which, using the standard parametrization of mixing matrices, are summarized as follows:

$$\theta_{12}^{PMNS} + \theta_{12}^{CKM} \sim \pi/4, \quad \theta_{23}^{PMNS} + \theta_{23}^{CKM} \sim \pi/4. \quad (1.1)$$

The previous structure, which is presumed to exist behind such empirical relations, is known as *quark-lepton complementarity (QLC)* and, while being appealing from a theoretical and phenomenological point of view, does not give any clue on which kind of symmetry could be responsible for them.

The usual answer to this problem is grand unification (GUT) in which quarks and leptons are unified into the same multiplets [2–8]; on the other hand, in non-GUT scenarios, one is somehow forced to input the CKM (PMNS) matrix into the relations that define the PMNS (CKM). Several authors have explored such a possibility [1, 9–15] and discussed the observable consequences of scenarios leading to QLC [16–20], including the effect of the RGE running on the stability of eq.(1.1) [21–24]. An extension of eq.(1.1) to the (13) sector results in a complete failure, as the sum $\theta_{13}^{PMNS} + \theta_{13}^{CKM} \sim 10^\circ$; thus, it is necessary to find a new connection between neutrinos and quarks that involves the reactor angle. The most promising suggestion is, once again, GUT-inspired and reads:

$$\theta_{13}^{PMNS} = \alpha \theta_{12}^{CKM}, \quad (1.2)$$

where α can be any $\mathcal{O}(1)$ number [10, 25–28]. One possibility to recover eq.(1.2) is to assume that the mixing matrices are related through:

$$U_{PMNS} \sim V_{CKM} T, \quad (1.3)$$

where T is an appropriate unitary matrix that we parametrize as the product of three sub-rotations:

$$T \equiv U_{23} U_{13} U_{12}. \quad (1.4)$$

In this paper we want to elaborate more on eq.(1.3), finding the exact theoretical relation among U_{PMNS} and V_{CKM} allowed by specific ansatz on the diagonalization procedure of the fermion mass matrices. This involves the determination of the matrix T ; by assuming an initial form for T of Bimaximal (BM), Tri-Bimaximal (TBM) [29] and Golden Ratio (GR) type [30], we compute in a systematic way all relevant corrections that allow to reproduce the neutrino mixing angles as well as the Jarlskog invariant [31]. Instead of performing an overall fit involving general perturbations of BM, TBM and GR mixings, we preferred to introduce three different corrections, one for each U_{ij} quoted in eq.(1.4), and study the prediction of mixing parameters determined by each of them. In this way, we are able to keep track of the relevant source of deviations from the initial form for T that allows a good fit to the experimental data. We find

that a complex parameter u is needed in the U_{13} rotation to increase the amount of leptonic CP violation up to the current experimental values while a simple real correction in the (12) plane is mandatory to account for the solar angle. Finally, deviation to maximality for the atmospheric angle can be accounted by a real shift ω in the (23) sector. In addition to mixing parameters, the newly found corrections are also compatible with the solar and atmospheric mass differences to a high degree of precision.

The paper is organized as follows: in Sect.(2) we discuss all the above-mentioned corrections in detail, showing how to include them in a perturbative approach to the determination of the mixing parameters; in Sect.(3) we show how to reproduce the experimental mass differences within our framework for all perturbed mixing patterns; finally, Sect.(4) is devoted to our conclusions. We close the paper with the Appendix where we report the expressions of the mixing parameters up to $\mathcal{O}(\lambda^3)$.

2 Corrections to BM, TBM and GR

2.1 Notation

Let us first fix our notation; we are working in the left-right (LR) basis and, with no loss of generality, we assume diagonal heavy right-handed neutrinos $M_R = M_R^{diag}$ and diagonal charged leptons $M_\ell = M_\ell^{diag}$. The diagonalization of the Dirac neutrino mass is achieved through $W_L^\dagger m_{\nu D} U_R = m_{\nu D}^{diag}$, so that the hermitean matrix $m_{\nu D} m_{\nu D}^\dagger$ is such that $W_L^\dagger m_{\nu D} m_{\nu D}^\dagger W_L = (m_{\nu D}^{diag})^2$, where the eigenvalues of $(m_{\nu D}^{diag})^2$ are real and non-negative, and the columns of W_L are the eigenvectors of the $m_{\nu D} m_{\nu D}^\dagger$ matrix. Applying the see-saw formula in the LR basis, we get:

$$\begin{aligned} m_\nu &= -m_{\nu D} (M_R^{diag})^{-1} m_{\nu D}^T \\ &= W_L m_{\nu D}^{diag} U_R^\dagger (M_R^{diag})^{-1} U_R^* m_{\nu D}^{diag} W_L^T. \end{aligned} \quad (2.1)$$

At this point, the matrix $m_0 = m_{\nu D}^{diag} U_R^\dagger (M_R^{diag})^{-1} U_R^* m_{\nu D}^{diag}$ is a complex symmetric matrix and, thus, it can be diagonalized by an unitary matrix T such that:

$$m_0 = T S T^T, \quad (2.2)$$

where S is a diagonal matrix with, in principle, complex entries. Thus, for the light neutrino mass we have the following decomposition:

$$m_\nu = -W_L T S T^T W_L^T. \quad (2.3)$$

To get the proper structure of U_{PMNS} , we assume a neutrino change of basis of the following type:

$$\nu' = U_{PMNS} \nu, \quad (2.4)$$

where the mass eigenstate are those indicated with ν . At the Lagrangian level, the symmetric mass term, in the basis of interaction eigenstates, is as follows:

$$(\nu^T)' m_\nu \nu' = \nu^T U_{PMNS}^T m_\nu U_{PMNS} \nu \equiv \nu^T m_\nu^{diag} \nu \quad (2.5)$$

so that:

$$m_\nu = U_{PMNS}^\star m_\nu^{diag} U_{PMNS}^\dagger, \quad (2.6)$$

and we can identify:

$$U_{PMNS} = W_L^\star T^\star \quad (2.7)$$

and

$$m_\nu^{diag} = S. \quad (2.8)$$

In the following we will assume $W_L \equiv V_{CKM}$, whose structure in the Wolfenstein parameterization is reported below:

$$V_{CKM} = \begin{pmatrix} 1 - \lambda^2/2 & \lambda & A\lambda^3(-i\eta + \rho) \\ -\lambda & 1 - \lambda^2/2 & A\lambda^2 \\ A\lambda^3(1 - i\eta - \rho) & -A\lambda^2 & 1 \end{pmatrix}. \quad (2.9)$$

The values of the V_{CKM} parameters used in our simulations are provided in Tab.(1). For the T

Parameter	Best-fit value and 1σ range
λ	0.2251 ± 0.0008
A	0.828 ± 0.01
η	0.355 ± 0.009
ρ	0.164 ± 0.009

Table 1: *Best-fit value and 1σ range of the V_{CKM} parameters, from [32].*

matrix, instead, one can in principle assume an exact Tri-Bimaximal mixing (TBM), Bimaximal mixing (BM) or Golden Ratio (GR) forms:

$$U_{BM} = \begin{pmatrix} \frac{1}{\sqrt{2}} & -\frac{1}{\sqrt{2}} & 0 \\ \frac{1}{2} & \frac{1}{2} & \frac{1}{\sqrt{2}} \\ -\frac{1}{2} & -\frac{1}{2} & \frac{1}{\sqrt{2}} \end{pmatrix} \quad U_{TBM} = \begin{pmatrix} \sqrt{\frac{2}{3}} & \frac{1}{\sqrt{3}} & 0 \\ -\frac{1}{\sqrt{6}} & \frac{1}{\sqrt{3}} & \frac{1}{\sqrt{2}} \\ \frac{1}{\sqrt{6}} & -\frac{1}{\sqrt{3}} & \frac{1}{\sqrt{2}} \end{pmatrix} \quad U_{GR} = \begin{pmatrix} \frac{c_{12}}{\sqrt{2}} & \frac{s_{12}}{\sqrt{2}} & 0 \\ \frac{s_{12}}{\sqrt{2}} & -\frac{c_{12}}{\sqrt{2}} & \frac{1}{\sqrt{2}} \\ \frac{s_{12}}{\sqrt{2}} & -\frac{c_{12}}{\sqrt{2}} & -\frac{1}{\sqrt{2}} \end{pmatrix} \quad (2.10)$$

Parameter	Best-fit value and 1σ range
$r \equiv \Delta m_{\text{sol}}^2 / \Delta m_{\text{atm}}^2 $	0.0295 ± 0.0008
$\tan(\theta_{12})$	0.666 ± 0.019
$\sin(\theta_{13})$	0.149 ± 0.002
$\tan(\theta_{23})$	0.912 ± 0.035
J_{CP}	-0.027 ± 0.010

Table 2: *Neutrino observables and their 1σ ranges as derived from NuFIT 5.3 [33, 34], using the dataset with SK atmospheric data [35]. For the extraction of the best-fit value and 1σ uncertainty of the Jarlskog invariant, we refer to its one-dimensional χ^2 projection from NuFIT 5.3.*

where $c_{12} = \cos \theta_{12}$, $s_{12} = \sin \theta_{12}$ and $\tan \theta_{12} = 1/\phi$, with $\phi = (1 + \sqrt{5})/2$. However, it turns out that the U_{PMNS} implied by them is unsatisfactory in the predicted values of the mixing angles and Jarlskog invariant J_{CP} , for which we use the following expression:

$$J_{\text{CP}} = \text{Im} [(U_{PMNS})_{11}(U_{PMNS})_{12}^*(U_{PMNS})_{21}^*(U_{PMNS})_{22}] . \quad (2.11)$$

We have summarized the situation in Tab.(3) where, for each mixing pattern, we have reported the perturbative prediction on $\sin(\theta_{13})$, $\tan(\theta_{12})$, $\tan(\theta_{23})$ (up to $\mathcal{O}(\lambda)$) and J_{CP} (up to $\mathcal{O}(\lambda^3)$). In the last column we have computed the *distance* Δ between such predictions and the current experimental values for a Normal Ordering (NO) of the neutrino masses¹, reported in Tab.(2). Such a *distance* is computed according the following formula:

$$\Delta = \sum_{i=1}^3 \left[\frac{P_i - B_i}{\sigma_i} \right]^2 , \quad (2.12)$$

where \vec{P} is a vector of parameters $\vec{P} = [\tan(\theta_{12}), \tan(\theta_{13}), \tan(\theta_{23}), J_{\text{CP}}]$ as predicted by TBM, BM and GR (see Tab.(3)), $\vec{\sigma}$ are the related 1σ errors and \vec{B} contains the best-fit values of Tab.(2), $\vec{B} = [\tan^{bf}(\theta_{12}), \tan^{bf}(\theta_{13}), \tan^{bf}(\theta_{23}), J_{\text{CP}}^{bf}]$. Δ allows us to estimate how far a given texture is from the current values of the mixing parameters.

While all patterns predict maximal (23) mixing and the same $\sin(\theta_{13})$, the differences come from J_{CP} (strongly suppressed for all patterns) and from the solar sector; in particular, for the latter the BM mixing results in a better agreement with the current experimental value than TBM and GR, as evident by the smaller Δ . The predictions in Tab.(3) are also reported in Fig.(1), together with their 1σ experimental spread (red rectangles)². From this we learn that, after the shifts of $\mathcal{O}(\lambda)$ provided by V_{CKM} , negative corrections are needed for all patterns to

¹For our purposes, it is enough to consider the normal hierarchy only, as the only significant difference with respect to the inverted ordering case is a slight preference for the opposite θ_{23} octant.

²We do not report the spread of J_{CP} as, for any patters, its absolute value is around two orders of magnitude smaller than the experimental best-fit.

T	$\sin(\theta_{13})$	$\tan(\theta_{12})$	$\tan(\theta_{23})$	J_{CP}	Δ
U_{TBM}	$\frac{\lambda}{\sqrt{2}}$	$\frac{1}{\sqrt{2}} + \frac{3\lambda}{2\sqrt{2}}$	1	$-\frac{1}{6}A\eta\lambda^3$	2715
U_{BM}	$\frac{\lambda}{\sqrt{2}}$	$1 - \sqrt{2}\lambda$	1	$\frac{1}{4\sqrt{2}}A\eta\lambda^3$	2500
U_{GR}	$\frac{\lambda}{\sqrt{2}}$	$\frac{2\sqrt{5}}{5+\sqrt{5}} + \frac{5\sqrt{2}}{5+\sqrt{5}}\lambda$	1	$-\frac{1}{2\sqrt{10}}A\eta\lambda^3$	2580

Table 3: *Perturbative predictions on $\sin(\theta_{13})$, $\tan(\theta_{12})$, $\tan(\theta_{23})$ (up to $\mathcal{O}(\lambda)$) and J_{CP} (up to $\mathcal{O}(\lambda^3)$) as obtained from the ansatz $U_{PMNS} = V_{CKM}^* T^*$, where T can be TBM, BM and GR mixing patterns. In the last column we report the values of the variable Δ defined in eq.(2.12).*

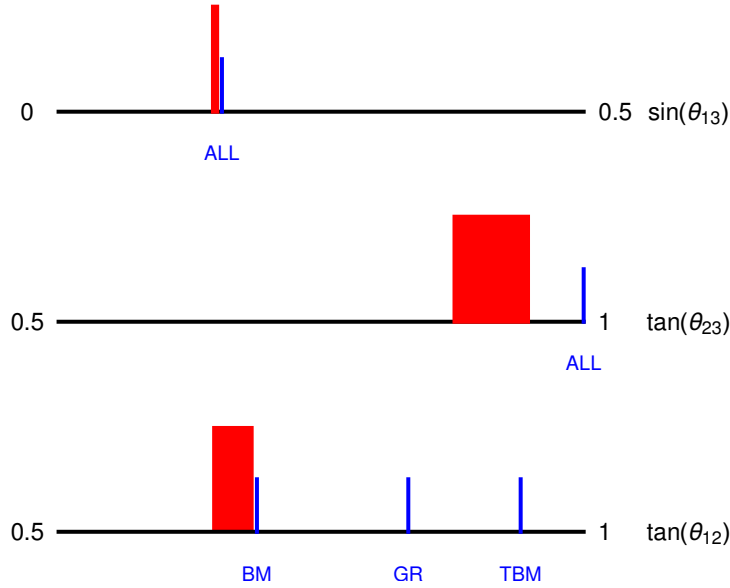


Figure 1: *Current 1σ experimental spread on $\tan(\theta_{12})$, $\tan(\theta_{23})$ and $\sin(\theta_{13})$ (red rectangles) and the predictions derived from $U_{PMNS} = V_{CKM}^* T^*$, where T can be TBM, BM and GR mixing patterns.*

jump into the 1σ allowed range for all mixing angles. It is worth to mention that, if 3σ allowed ranges for the atmospheric mixing angle and the Jarlskog invariant are taken into account, the BM scenario is compatible with experimental data. Indeed, both $\sin \theta_{23} \sim 1$ and $J_{CP} \sim 0$ are not yet excluded by neutrino experiments [34].

In the next section we will analyze, in a systematic way, which corrections of U_{ij} in eq.(1.4) are the most appropriate to better fit the neutrino mixing parameters.

2.2 Corrections from the (13)-sector to BM, TBM and GR

We start our analysis by studying in detail the correction to the standard patterns from the (13)-sector. The main idea is that, given the absence of any CP phase in (2.10), eq.(2.7) implies a very low CP violation in the lepton sector [36], of the order of $\mathcal{O}(\lambda^3)$ and proportional to

η as shown from the expressions of J_{CP} in Tab.(2). Thus, to allow for a larger CP violation, which seems to be preferred by recent oscillation results, new sources of symmetry violation are needed. Assuming for T the decomposition as in eq.(1.4), larger CP violation can be generated by slightly shifting the (13)-rotation from the identity; to this aim, we introduce a complex parameter u [37] such that $|u| \ll 1$ and we rescale it by one power of the Cabibbo angle λ . This also implies that the rescaled $|u| \sim \mathcal{O}(1)$. Thus, the (13)-rotation has the following structure:

$$U_{13} = \begin{pmatrix} 1 - \frac{\lambda^2}{2}|u|^2 & 0 & u\lambda \\ 0 & 1 & 0 \\ -u^*\lambda & 0 & 1 - \frac{\lambda^2}{2}|u|^2 \end{pmatrix}. \quad (2.13)$$

To construct completely the matrix T , we need to specify the rotations in the other two sectors, the (12) and (23)-rotations. In order to contemplate the BM, TBM and GR mixings simultaneously, we leave unspecified the rotation in the (12)-sector and, since the sign of such a rotation is not fixed a priori, we leave it as free, encoding this uncertainty into the parameter σ , that can assume values ± 1 . At this stage, the rotation in the (23)-sector is maximal (so, from our ansatz, we expect all deviations to θ_{23} coming from V_{CKM} , see below). Thus, we have:

$$U_{23} = \begin{pmatrix} 1 & 0 & 0 \\ 0 & \frac{1}{\sqrt{2}} & \frac{1}{\sqrt{2}} \\ 0 & -\frac{1}{\sqrt{2}} & \frac{1}{\sqrt{2}} \end{pmatrix}, \quad U_{12} = \begin{pmatrix} \tilde{c}_{12} & \sigma \tilde{s}_{12} & 0 \\ -\sigma \tilde{s}_{12} & \tilde{c}_{12} & 0 \\ 0 & 0 & 1 \end{pmatrix}, \quad (2.14)$$

where $\tilde{c}_{12} \equiv \cos(\tilde{\theta}_{12})$, $\tilde{s}_{12} \equiv \sin(\tilde{\theta}_{12})$ are the cosinus and sinus functions of a rotation in the (12)-sector (not to be confused with the usual solar angle). This, in turn, implies the following structure of the T matrix:

$$T \equiv U_{23}U_{13}U_{12} = \begin{pmatrix} \tilde{c}_{12} \left(1 - \frac{\lambda^2}{2}|u|^2\right) & \sigma \tilde{s}_{12} \left(1 - \frac{\lambda^2}{2}|u|^2\right) & u\lambda \\ -(\sigma \tilde{s}_{12} + \tilde{c}_{12}u^*\lambda)/\sqrt{2} & (\tilde{c}_{12} - \sigma \tilde{s}_{12}u^*\lambda)/\sqrt{2} & \left(1 - \frac{\lambda^2}{2}|u|^2\right)/\sqrt{2} \\ (\sigma \tilde{s}_{12} - \tilde{c}_{12}u^*\lambda)/\sqrt{2} & -(\tilde{c}_{12} + \sigma \tilde{s}_{12}u^*\lambda)/\sqrt{2} & \left(1 - \frac{\lambda^2}{2}|u|^2\right)/\sqrt{2} \end{pmatrix}. \quad (2.15)$$

Notice that unitarity is fully respected up to $\mathcal{O}(\lambda^3)$. With our parametrization, the relevant patterns are recovered once we fix $u = 0$ (for all of them) and $\tilde{s}_{12} = 1/\sqrt{3}$, $\tilde{c}_{12} = 1/\sqrt{2}$ and $\tilde{s}_{12}^2 = 2/(5 + \sqrt{5})$ for TBM, BM and GR, respectively (at this stage, the value of σ is irrelevant). For the Jarlskog invariant J_{CP} , up to $\mathcal{O}(\lambda^3)$, we get the expression as below:

$$J_{\text{CP}} = \frac{\lambda}{4} \sigma \text{Im}(u) \sin(2\tilde{\theta}_{12}) + \frac{\lambda^2}{2\sqrt{2}} \text{Im}(u) \cos(2\tilde{\theta}_{12}) + \\ - \frac{\lambda^3}{8} \sigma \sin(2\tilde{\theta}_{12}) \left[\sqrt{2}A\eta + 2\text{Im}(u) \left(2 + |u|^2 + \sqrt{2}\text{Re}(u) \right) \right]. \quad (2.16)$$

Some comments are in order:

- in the limit of exact TBM, BM and GR, the invariant J reduces to:

$$J_{\text{CP}}^{\text{TBM}} = -\frac{A\eta\lambda^3\sigma}{6}, \quad J_{\text{CP}}^{\text{BM}} = -\frac{A\eta\lambda^3\sigma}{4\sqrt{2}}, \quad J_{\text{CP}}^{\text{GR}} = -\frac{A\eta\lambda^3\sigma}{2\sqrt{10}}, \quad (2.17)$$

which all lead to a suppressed CP violation in the lepton sector, in agreement with Tab.(3) for an appropriate choice of σ ;

- retaining terms proportional to $\text{Re}(u)$ (and setting $\text{Im}(u) = 0$) does not cure the previous problem since they appear only to $\mathcal{O}(\lambda^3)$;
- to reconcile our prediction with the experimental value, we need to allow a deviation from exact TBM, BM and GR forms provided by $\text{Im}(u)$. The $\mathcal{O}(\lambda)$ degeneracy between σ and $\text{Im}(u)$ will allow the latter to assume both positive and negative values.

To find the set of values of $\text{Re}(u)$, $\text{Im}(u)$ that allows to reproduce the best fit point of J_{CP} ($J_{\text{CP}}^{\text{bf}}$), in Fig.(2) we plot the ensemble of u values which makes the modified versions of TBM (black solid line), BM (red dashed line) and GR (blue dot-dashed line) compatible with $J_{\text{CP}}^{\text{bf}}$ at 1σ , subject to the constraint $|u| < 1$. Given the similarities in the analytical structure of TBM, BM and GR, we see that overlapping complex u -region are covered; in addition, as commented above, we also expect a less relevant dependence on $\text{Re}(u)$ compared to $\text{Im}(u)$. The main conclusion is that $|\text{Im}(u)| \gtrsim 0.3$ (and almost any $\text{Re}(u)$ in the $[-1, 1]$ range) is enough to get the correct amount of leptonic CP violation, for any choice of the starting matrix. The mild $\text{Re}(u)$, $\text{Im}(u)$ correlation is mainly dictated by the constraint $|u| < 1$.

Now we go for the expressions of the mixing angles. For the reactor angle we get a formula which is independent on the $\tilde{\theta}_{12}$ parameter (and thus on the sign of σ) up to $\mathcal{O}(\lambda^3)$ terms

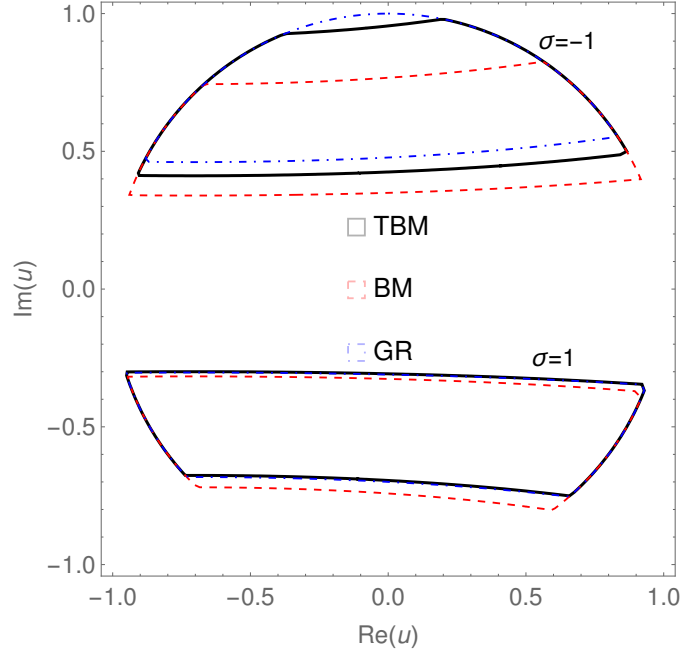


Figure 2: *Ensemble of u values which make the modified versions of TBM (black solid line), BM (red dashed line) and GR (blue dot-dashed line) compatible with $J_{\text{CP}}^{\text{bf}}$ at 1σ . The upper (lower) plots show the solutions obtained with $\sigma = -1$ ($\sigma = +1$).*

(notice that $\mathcal{O}(\lambda^2)$ terms vanish):

$$\sin(\theta_{13}) = \sqrt{1/2 + |u|^2 + \sqrt{2}\text{Re}(u)\lambda + \frac{[2\sqrt{2}A\rho - 4A\eta\text{Im}u + (-2 + 4A\rho)\text{Re}u - |u|^2(3\sqrt{2} + 2\text{Re}(u))]}{4\sqrt{1 + 2|u|^2 + 2\sqrt{2}\text{Re}(u)}}\lambda^3}. \quad (2.18)$$

In the limit of exact TBM, BM and GR mixing ($u = 0$), we recover the well-known relation $\sin(\theta_{13}) = \frac{\lambda}{\sqrt{2}} + \mathcal{O}(\lambda^3)$, which is still a good approximation, see also Tab.(3). Moreover, eq.(2.18) shows that, barring accidental cancellations, negative $\text{Re}(u)$ values are needed to compensate for positive shifts driven by $|u|$ (unless $\text{Im}(u)$ is also small, in that case small positive values of $\text{Re}(u)$ are also allowed).

Not too much must be said for the atmospheric angle; up to $\mathcal{O}(\lambda^3)$ we get:

$$\tan(\theta_{23}) = 1 + \frac{\lambda^2}{2} [-1 + 4A - 2\sqrt{2}\text{Re}(u)]. \quad (2.19)$$

The most interesting feature is the absence of any dependence on $\text{Im}(u)$; thus, the small deviations from maximality are governed, beside the Cabibbo angle, by $\text{Re}(u)$ only. We also have to mention that the current best fit point is away from maximal mixing at the level of 3σ , see Tab.(2). Thus, relatively large positive $\text{Re}(u)$ are needed to shift $\tan(\theta_{23})$ towards its 1σ preferred value which lies around $\tan(\theta_{23})^{bf} \sim 0.9$. As in the previous case, no dependence on $\tilde{\theta}_{12}$ appears so that exact TBM, BM and GR hypothesis give the same expression in eq.(2.19) with $\text{Re}(u) = 0$.

Finally, for the solar angle we get:

$$\begin{aligned} \tan(\theta_{12}) = & \tan(\tilde{\theta}_{12}) + \frac{\lambda}{\sqrt{2}\tilde{c}_{12}^2}\sigma + \frac{\lambda^2}{2\tilde{c}_{12}^3}\tilde{s}_{12} + \\ & + \frac{\lambda^3}{4\tilde{c}_{12}^4}\sigma [\sqrt{2}(1 - 2A\tilde{c}_{12}^2\rho) + \tilde{c}_{12}^2(\sqrt{2}|u|^2 + 2\text{Re}(u))]. \end{aligned} \quad (2.20)$$

The most considerable feature is that the corrections implied by U_{13} of eq.(2.13) are too small to be significant; thus, the expressions of θ_{12} are very similar to those quoted in Tab.(3). In addition, once we specify the values of $\tilde{\theta}_{12}$ for the relevant patterns, there are no free parameters up to $\mathcal{O}(\lambda^2)$; we can then derive the following sum-rules among physical angles (that, for the sake of simplicity, we report here up to first order in $\sin(\theta_{13})$):

$$\tan(\theta_{12}) = \begin{cases} \frac{1}{\sqrt{2}} + 3\sigma \sin(\theta_{13})/2 & \text{for TBM} \\ 1 + 2\sigma \sin(\theta_{13}) & \text{for BM} \\ 2\sqrt{5}/(5 + \sqrt{5}) + 10\sigma \sin(\theta_{13})/(5 + \sqrt{5}) & \text{for GR.} \end{cases} \quad (2.21)$$

The only possibility to (marginally) reconcile the previous sum rules with the experimental value happens for BM mixing with $\sigma = -1$, which shows a deviation from $\tan(\theta_{12})^{bf}$ at around $\sim 3\%$ (compare with Fig.(1)); for the other mixing patterns, this difference amounts to values

as large as $\sim 20\%$ for GR and $\sim 30\%$ for TBM. To better quantify the (dis-)agreements of the obtained U_{PMNS} with the experimental data after including the corrections in eq.(2.13), we perform a simple χ^2 test, with the function:

$$\chi^2 = \frac{[J_{\text{CP}} - J_{\text{CP}}^{bf}]^2}{\sigma_{J_{\text{CP}}}^2} + \frac{[\sin(\theta_{13}) - \sin(\theta_{13})^{bf}]^2}{\sigma_{\sin(\theta_{13})}^2} + \frac{[\tan(\theta_{23}) - \tan(\theta_{23})^{bf}]^2}{\sigma_{\tan(\theta_{23})}^2} + \frac{[\tan(\theta_{12}) - \tan(\theta_{12})^{bf}]^2}{\sigma_{\tan(\theta_{12})}^2} \quad (2.22)$$

For all patterns, the minimum of the χ^2 is very large, in the range $(10 - 10^3)$ and it is dominated by the $\tan(\theta_{12})$ term; in fact, if we exclude θ_{12} from the χ^2 function, the fit improves considerably for all patterns, with $\chi_{\min}^2 \sim \mathcal{O}(20)$ (the best performance being obtained by BM mixing with $\sigma = -1$). The problem related to the deviation from maximality of θ_{23} is, instead, less relevant because of a larger relative 1σ error compared to θ_{12} . Finally, the corrections analyzed here help in improving the values of Δ , $\Delta = (2708, 2492, 2573)$ for TBM, BM and GR mixings, respectively. Obviously, assuming for the variable u a smaller value, that is shifting $u \rightarrow \lambda^N u$, does not solve the problem for any integer N .

2.3 Perturbation on the (23)- sector

One possibility to alleviate the problem in the (23)-sector is to slightly modify U_{23} of eq.(1.4) by inserting a new real parameter ω according to³:

$$U_{23} = \begin{pmatrix} 1 & 0 & 0 \\ 0 & \frac{1}{\sqrt{2}} - \lambda\omega - \sqrt{2}\lambda^2\omega^2 - 2\lambda^3\omega^3 & \frac{1}{\sqrt{2}} + \omega\lambda \\ 0 & -\frac{1}{\sqrt{2}} - \omega\lambda & \frac{1}{\sqrt{2}} - \lambda\omega - \sqrt{2}\lambda^2\omega^2 - 2\lambda^3\omega^3 \end{pmatrix}. \quad (2.23)$$

Notice that, to maintain the unitarity of U_{23} , we displayed up to $\mathcal{O}(\lambda^3)$ terms. We repeat the same calculations as before and indicate with a *prime* the new expressions of the mixing parameters while leaving *unprimed* the results of the previous section. The relevant corrections driven by ω are as follows:

$$\begin{aligned} J'_{\text{CP}} &= J_{\text{CP}} - \frac{\lambda^3}{2} \text{Im}(u) \left[\omega \cos(2\tilde{\theta}_{12}) + 2\sigma\omega^2 \sin(2\tilde{\theta}_{12}) \right] \\ \sin'(\theta_{13}) &= \sin(\theta_{13}) + \frac{\lambda^2\omega}{\sqrt{2}} \frac{[\sqrt{2} + 2\text{Re}(u)]}{\sqrt{1 + 2|u|^2 + 2\sqrt{2}\text{Re}(u)}} \\ \tan'(\theta_{23}) &= \tan(\theta_{23}) + 2\sqrt{2}\lambda\omega \\ \tan'(\theta_{12}) &= \tan(\theta_{12}) - \frac{\lambda^2\omega\sigma}{\cos^2(\tilde{\theta}_{12})}. \end{aligned} \quad (2.24)$$

We see that $J_{\text{CP}}, \theta_{12}$ and θ_{13} acquire small $\mathcal{O}(\lambda^{2-3})$ corrections that do not improve the fit compared to the previous section. For the atmospheric angle, instead, an $\mathcal{O}(\lambda)$ is relevant,

³Since the complex variable u was already enough to guarantee the correct amount of leptonic CP violation, we prefer to reduce the number of free parameters choosing a real correction ω .

especially for negative values of ω as, starting from maximality, we need a negative correction to jump into the experimental value⁴. Notice that this is true for any value of σ . However, even though the atmospheric angle turns out to be in the correct range, the fits to the expressions in eq.(2.24) are only slightly improved but still remain $\gtrsim \mathcal{O}(100)$ because of the poor foreseen solar angle; as before, only the modified BM mixing case presents a good minimum of the χ^2 at $\chi_{min}^2 = 3.47$. For the sake of illustration, the behaviour of the $\Delta\chi^2 = \chi^2 - \chi_{min}^2$ as a function of ω is presented in Fig.(3). For every ω , we have marginalized over $\text{Re}(u)$ and $\text{Im}(u)$ in the fit.

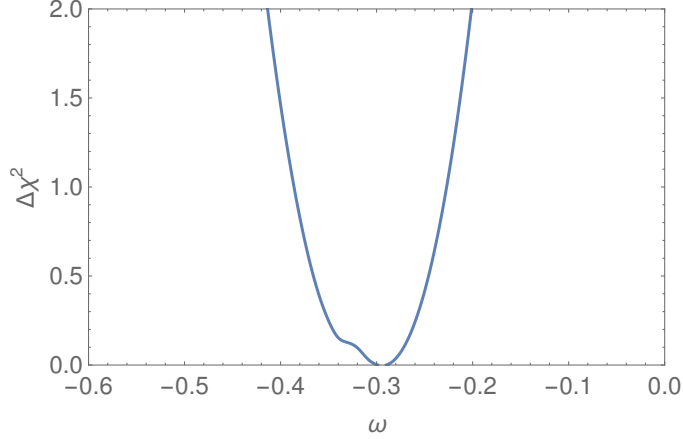


Figure 3: $\Delta\chi^2 = \chi^2 - \chi_{min}^2$ behaviour as a function of ω for the modified BM mixing. In the fit procedure, we have marginalized over the $(\text{Re}(u), \text{Im}(u))$ pair.

2.4 The full glory: perturbation on the (12)- sector

The results of the previous sections have shown that the predictions for J_{CP} and $\sin(\theta_{13})$ are good for all mixing once the u -corrections are included. The ω corrections are needed to reconcile the θ_{23} deviations from maximal mixing (common to all patterns) while the solar angle remains sensitively away from its experimental value for TBM and GR mixing but sufficiently close to it for BM. Thus, in order to complete our program to match the data of Tab.(2), we need to add a (real) correction of $\mathcal{O}(\lambda)$ to the (12)-sector, that we dub with z . We parameterize it in the following way:

$$U_{12} = \begin{pmatrix} K & \tilde{s}_{12}\sigma + z\lambda & 0 \\ -\tilde{s}_{12}\sigma - z\lambda & K & 0 \\ 0 & 0 & 1 \end{pmatrix}, \quad (2.25)$$

where $K = \tilde{c}_{12} - \tilde{s}_{12}z\sigma/\tilde{c}_{12}\lambda - z^2/(2\tilde{c}_{12}^3)\lambda^2 - \tilde{s}_{12}z^3\sigma/(2\tilde{c}_{12}^5)\lambda^3$. The expression of the mixing parameters are modified accordingly; in particular, θ_{13} and θ_{23} are unaffected by z , so their

⁴The three main neutrino global fits [33, 38, 39] do not agree on the preferred θ_{23} octant, even though the 3σ ranges are all compatible. In our analysis, an higher octant value for θ_{23} can be easily obtained with a positive ω value.

expressions of eq.(2.24) are valid even in this case. The Jarlskog invariant gets an $\mathcal{O}(\lambda^2)$ correction of the form:

$$J_{\text{CP}}'' = J_{\text{CP}}' + \frac{\lambda^2}{2} \frac{\cos(2\tilde{\theta}_{12})\text{Im}(u)}{\cos(\tilde{\theta}_{12})} z. \quad (2.26)$$

By construction, the most interesting case is related to θ_{12} ; here, corrections of $\mathcal{O}(\lambda)$ driven by z compete with that shown in eq.(2.20):

$$\tan''(\theta_{12}) = \tan(\theta_{12})' + \lambda \frac{\sigma z}{\cos^3(\tilde{\theta}_{12})}. \quad (2.27)$$

Thus, we expect that a cancellation among the λ coefficients could bring the TBM and GR mixing in agreement with the data (for any σ) while for BM the contribution from z (and $\sigma = -1$) must be small in order not to destroy the agreement found above; conversely, we expect that $\sigma = 1$ will be acceptable for non-vanishing z corrections. To check whether this is the case, we minimized the χ^2 function of eq.(2.22) over the four independent parameters $\text{Re}(u)$, $\text{Im}(u)$, ω and z and reported their best fit values in Tab.(4). For all patterns, the minimum of the χ^2 is

Pattern	$\text{Re}(u)$	$\text{Im}(u)$	ω	z
TBM	-0.27(-0.27)	0.57(-0.55)	-0.27(-0.27)	-0.50(-0.77)
BM	-0.27(-0.29)	0.57(-0.56)	-0.27(-0.27)	0.08(-1.17)
GR	-0.27(-0.27)	0.57(-0.54)	-0.27(-0.27)	-0.73(-0.55)

Table 4: Values of the parameters $\text{Re}(u)$, $\text{Im}(u)$, ω and z that minimize the χ^2 function of eq.(2.22), computed for $\sigma = -1$ and, in parenthesis, for $\sigma = 1$. For all patterns, $\chi_{\min}^2 \sim 0$.

very close to zero, so we did not report it on the table. As expected, the magnitude and signs of the needed z 's reflects our considerations below eq.(2.27). In addition, the very similar values for $\text{Re}(u)$ and $\text{Im}(u)$ can be understood from Fig.(2), where the acceptable regions for such parameters are almost equivalent for each pattern. Finally, compared to the previous section, the value of ω is compatible with the BM case previously analyzed and, as expected, tends to assume a very similar strength for all other patterns and signs of σ ($\mathcal{O}(\lambda)$ corrections are universal). The 90% and 99% confidence levels of the χ^2 function in the (ω, z) -plane for TBM (left panel), BM (middle panel) and GR (right panel) are reported in Fig.(4); in each plots we included both ± 1 possibilities for σ and marginalized over the $(\text{Re}(u), \text{Im}(u))$ pair.

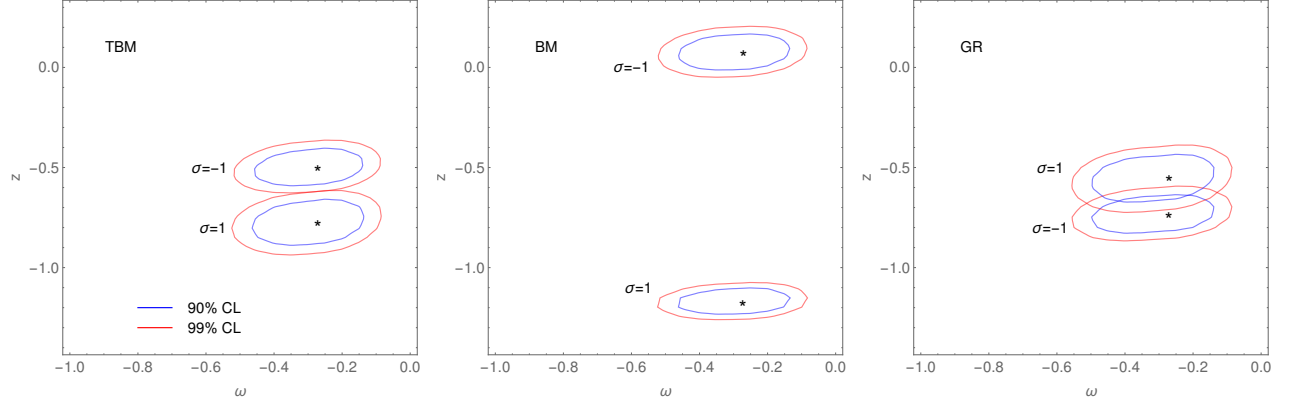


Figure 4: The 90% and 99% χ^2 confidence levels in the (ω, z) -plane for TBM (left panel), BM (middle panel) and GR (right panel). In each plots, we have reported both ± 1 possibilities for σ and marginalized over the $(\text{Re}(u), \text{Im}(u))$ pair.

3 On the neutrino masses

The next step is to ensure that our procedure is able to reproduce the solar and atmospheric mass differences. Eq.(2.1) offers the structure of the neutrino mixing matrix in terms of a right rotation U_R (four real parameters), three right-handed neutrino masses and three Dirac neutrino masses, for a total of ten unknown parameters; of those, four have been used to constrain the matrix T in eq.(2.2), and the remaining six parameters are left to describe neutrino masses. To determine them, one can try to figure out the structure of the diagonal matrix S by inverting eq.(2.2), so that:

$$S = T^\dagger m_{\nu_D}^{diag} U_R^\dagger (M_R^{diag})^{-1} U_R^* m_{\nu_D}^{diag} T^*. \quad (3.1)$$

Notice that the matrix $S \equiv m_{\nu}^{diag}$ does not depend on the quark mixing. One possibility to determine the unknown parameters is to rephrase eq.(3.1) to the more useful form:

$$S - T^\dagger m_0 T^* = 0. \quad (3.2)$$

Its left-hand side is a symmetric matrix made complex by the entries of m_{ν}^{diag} and by the T matrix, needed to successfully reproduce the leptonic CP violation. Thus, eq.(3.2) is equivalent to 12 conditions, which have to be simultaneously valid. However, we can easily verify that the imaginary parts of the elements of T are always smaller than the real part (at the level of 20% or smaller) with a notable exception of the element (13), for which the imaginary part is either larger (in the only case when T is the corrected BM mixing with $\sigma = -1$) or just half of the real part. With the aim of catching the relevant physics, not obfuscated by useless details (phases are of the uttermost importance for CP violation, not for neutrino masses), we prefer to deal with real S and T matrices; this allows us to reduce the number of constraints to six only⁵. Even in this case, the large number of free parameters makes the expressions of

⁵If, instead, we prefer to deal with complex matrices, thus phases must be added to U_R that helps in making vanishing all imaginary parts of eq.(3.2).

neutrino masses quite cumbersome. Thus, we only give a numerical solution to eq.(3.2). For the S matrix we take the following expression, valid for the Normal Ordering (NO) case:

$$S = \text{diag}(m_1, \sqrt{m_1^2 + \Delta m_{\text{sol}}^2}, \sqrt{m_1^2 + \Delta m_{\text{atm}}^2}), \quad (3.3)$$

where m_1 is the absolute neutrino mass scale that, for the sake of simplicity, we assume vanishing. We then construct the *adimensional* function:

$$F(\vec{m}_{\nu_D}, \vec{M}_R, \vec{\theta}_R) = \frac{\sum_{j<i=1}^3 [S_{ij} - (T^T m_0 T)_{ij}]^2}{\Delta m_{\text{sol}}^2}, \quad (3.4)$$

and look for minima as close as possible to zero. Here the vectors have the following entries, with obvious meaning:

$$\vec{m}_{\nu_D} = (m_{\nu_{D_1}}, m_{\nu_{D_2}}, m_{\nu_{D_3}}) \quad \vec{M}_R = (M_{R_1}, M_{R_2}, M_{R_3}) \quad \vec{\theta}_R = (\theta_{R_{12}}, \theta_{R_{13}}, \theta_{R_{23}}). \quad (3.5)$$

We consider ourselves satisfied when $F(\vec{m}_{\nu_D}, \vec{M}_R, \vec{\theta}_R) < 1$, meaning that all the differences between the corresponding matrix elements of S and $T^T m_0 T$ are smaller than the smallest measured mass scale Δm_{sol}^2 . The minimization procedure has been carried out by means of the software MultiNest, which is based on nested sampling normally used for calculation of the Bayesian evidence [40–42]. The choice of priors in this context is relevant. To prove that a solution to the system (3.2) exists, we set:

$$1 \leq m_{\nu_{D_1}}/\text{GeV} < 10, \quad 10 \leq m_{\nu_{D_2}}/\text{GeV} < 100, \quad 100 \leq m_{\nu_{D_3}}/\text{GeV} < 500, \\ 10^{13} \leq M_{R_1}/\text{GeV} < 10^{14}, \quad 10^{14} \leq M_{R_2}/\text{GeV} < 10^{15}, \quad 10^{15} \leq M_{R_3}/\text{GeV} < 10^{16}, \quad (3.6)$$

$$\vec{\theta}_R \in [0, 2\pi).$$

Notice that, being the neutrino masses given by complicated expressions of parameters, the position $m_{\nu_{D_1}} < m_{\nu_{D_2}} < m_{\nu_{D_3}}$ and $M_{R_1} < M_{R_2} < M_{R_3}$ does not correspond a priori to a definite mass hierarchy, as it would be the case for a standard see-saw mechanisms where, for example, $m_i \sim m_{\nu_{D_i}}^2/M_{R_i}$ for NO. We have analyzed the 6 different cases corresponding to modified BM, TBM and GR and the two values of $\sigma = \pm 1$; for each texture, we reported in Tab.(5) the minimum of $F(\vec{m}_{\nu_D}, \vec{M}_R, \vec{\theta}_R)$ and the values of the vectors \vec{m}_{ν_D} , \vec{M}_R and $\vec{\theta}_R$ in which the minimum is assumed. We also report in Fig.(5) an example of posterior distributions for the BM case, $\sigma = -1$ (all cases are very similar to each other). Let us analyze more in detail the results of our minimizing procedure. First of all, none of the analyzed patterns can be tagged as a preferred one, as the minima of the F function are very close to each other. This is in agreement with what we found for the mixing angles where, after including all relevant corrections, no preferred choice emerged. The vector \vec{m}_{ν_D} is characterized by the fact that the first and third element prefer values at their upper and lower limits, respectively while

		F^{\min}	\vec{m}_{ν_D} (GeV)	\vec{M}_R (10^{13} GeV)	$\vec{\theta}_R$ ($^\circ$)
BM	$\sigma = +1$	0.42	(9.35, 55.35, 117.70)	(4.0, 70.10, 297.51)	(145.80, 195.44, 162.01)
	$\sigma = -1$	0.44	(9.98, 36.84, 111.52)	(3.59, 67.78, 708.16)	(122.88, 12.88, 112.59)
TBM	$\sigma = +1$	0.31	(9.38, 58.54, 130.56)	(3.41, 93.21, 794.35)	(331.00, 347.73, 317.70)
	$\sigma = -1$	0.34	(9.66, 34.52, 159.29)	(2.09, 55.69, 485.30)	(321.58, 354.03, 221.83)
GR	$\sigma = +1$	0.19	(9.83, 80.88, 201.77)	(3.55, 86.014, 728.73)	(341.65, 171.70, 188.76)
	$\sigma = -1$	0.45	(9.26, 42.48, 156.88)	(2.97, 38.95, 268.45)	(145.00, 8.15, 341.63)

Table 5: *Results of the minimization procedure of the function $F(\vec{m}_{\nu_D}, \vec{M}_R, \vec{\theta}_R)$ in eq.(3.4). F^{\min} stands for the minimum value of such a function; the meaning of the three vectors \vec{m}_{ν_D} , \vec{M}_R and $\vec{\theta}_R$ has been given in eq.(3.5).*

$m_{\nu_{D_2}}$ is generally confined in the central region (with an exception for the case TBM, $\sigma = +1$ which, instead, prefers larger values). As for the Majorana masses, we observe similarities in all elements among the different patterns: M_{R_1} and M_{R_3} tend to stay close to their allowed lower and upper bounds, respectively, while M_{R_2} is mostly concentrated in the middle region around $[40 - 90] \cdot 10^{13}$ GeV. It is interesting to observe that the posterior distributions (middle panels of Fig.(5)) are almost flat for M_{R_3} but peaked at large allowed values for M_{R_1} and M_{R_2} ; while for the latter case this seems consistent with the values at the minimum of F , for the former this behavior does not completely match what reported in Tab.(5). We interpret this as that M_{R_1} gives a smaller contribution to F as the other Majorana masses. This happens also for the first Dirac neutrino mass $m_{\nu_{D_1}}$, whose best fit value is close to its upper limit while the posterior distribution is essentially flat. Finally, a look at Fig.(5) reveals that the posterior distributions for the mixing angles are multi-modal; in particular, a clear bi-modal distribution is seen for $\theta_{R_{12}}$, around $|\sin(\theta_{R_{12}})| \sim 1/2$, and for $\theta_{R_{13}}$ around $|\sin(\theta_{R_{13}})| \sim 0$; this is also visible in Tab.(5). A less clear bi-modal behaviour is also present for $\theta_{R_{23}}$ but the spreads around the maximum posterior probability are not negligible. Assuming the fixed values $\sin(\theta_{R_{12}}) = 1/2$ and $\sin(\theta_{R_{13}}) = 0$, the right-handed rotation implied by our fit is as follows:

$$U_R = \begin{pmatrix} \sqrt{3}/2 & 1/2 & 0 \\ -c_{23}/2 & \sqrt{3}c_{23}/2 & s_{23} \\ s_{23}/2 & -\sqrt{3}s_{23}/2 & c_{23} \end{pmatrix}. \quad (3.7)$$

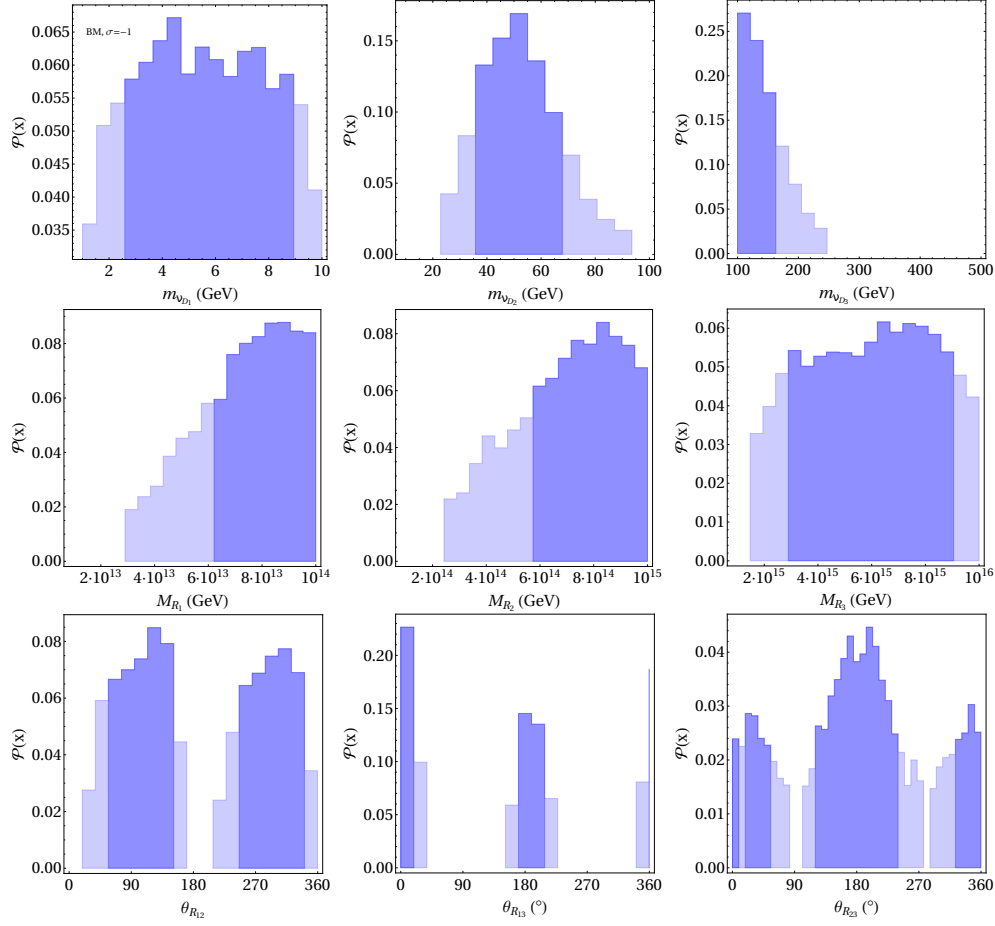


Figure 5: *Posterior distributions for the elements of the vectors \vec{m}_{ν_D} (first line) \vec{M}_R (middle line) and $\vec{\theta}_R$ (lower line) for the BM case, $\sigma = -1$. Darker and lighter blue refer to 68% and 95% credible intervals, respectively.*

4 Conclusions

In this paper we have investigated in detail the hypothesis that the PMNS mixing matrix is given by the relation $U_{PMNS} = V_{CKM}^* T^*$, where T is a unitary matrix. By considering the decomposition $T \equiv U_{23} U_{13} U_{12}$, we have shown that a T matrix coinciding with TBM, BM and GR mixing fails, among others, to reproduce the experimental preferred value of the Jarlskog invariant, which is related to the third power of the Cabibbo angle. To solve these issues, we have analyzed $\mathcal{O}(\lambda)$ corrections to the U_{ij} matrices, showing that a complex parameter u is needed in the (13) rotation to reconcile our ansatz with the experimental amount of leptonic CP violation. While a correction ω in the (23) sector is needed for a substantial deviation of the atmospheric angle from maximality, it only marginally improves the global fit to the experimental values of the mixing angles, because of a wrong estimate of θ_{12} in all cases but BM. Thus, a shift in the (12) plane is mandatory to account for the solar angle and, consequently, to get an excellent fit for all mixing parameters and for any initial choice of T . The

ansatz illustrated here is also appropriate to reproduce the value of solar and atmospheric mass differences. Indeed, equipped with the best fit values of the $\text{Re}(u)$, $\text{Im}(u)$, ω and z parameters, we have shown that a description of neutrino masses via the see-saw mechanism is possible. Because of the cumbersome analytical expressions of $\Delta m_{sol,atm}^2$, we relied on numerical scan of the vector components of \vec{m}_{ν_D} , \vec{M}_R and $\vec{\theta}_R$ of eq.(3.5) and found that, with our choice of priors, a complete description of neutrino masses and mixing under the assumption $U_{PMNS} = V_{CKM}^* T^*$ is possible.

Acknowledgments

We thank João Penedo and Matteo Parriciatu for useful comments and suggestions on our manuscript.

Appendix: Full $\mathcal{O}(\lambda^3)$ formulae

For the sake of completeness, we report here the full $\mathcal{O}(\lambda^3)$ expressions of the mixing parameters obtained from our ansatz $U_{PMNS} = V_{CKM}^* T^*$.

$$\begin{aligned}
J = & \frac{\lambda}{4} \sigma \text{Im}(u) \sin(2\tilde{\theta}_{12}) + \lambda^2 \frac{\text{Im}(u) \cos^2(\tilde{\theta}_{12})}{4 \cos(\tilde{\theta}_{12})} (\sqrt{2} \cos(\tilde{\theta}_{12}) + 2z) + \\
& - \frac{\lambda^3}{8} \sigma \sin(2\tilde{\theta}_{12}) [\sqrt{2} A \eta + 2 \text{Im}(u) (2 + |u|^2 + \sqrt{2} \text{Re}(u))] + \\
& - \frac{\lambda^3}{2} \text{Im}(u) [\omega \cos(2\tilde{\theta}_{12}) + 2\sigma \omega^2 \sin(2\tilde{\theta}_{12})] + \\
& - \lambda^3 z \sigma \left\{ -8\sqrt{2} \sin(\tilde{\theta}_{12}) \text{Im}(u) + \frac{2z \text{Im}(u) \sin(\tilde{\theta}_{12})}{\cos(\tilde{\theta}_{12})^3} [3 \cos^2(\tilde{\theta}_{12}) + \sin^2(\tilde{\theta}_{12})] \right\}
\end{aligned} \tag{4.1}$$

$$\begin{aligned}
\sin(\theta_{13}) = & \sqrt{1/2 + |u|^2 + \sqrt{2} \text{Re}(u)} \lambda + \\
& + \frac{\lambda^2 \omega}{\sqrt{2}} \frac{[\sqrt{2} + 2 \text{Re}(u)]}{\sqrt{1 + 2|u|^2 + 2\sqrt{2} \text{Re}(u)}} + \\
& + \lambda^3 \frac{[2\sqrt{2} A \rho - 4A \eta \text{Im} u + (-2 + 4A \rho) \text{Re} u - |u|^2 (3\sqrt{2} + 2 \text{Re}(u))]}{4\sqrt{1 + 2|u|^2 + 2\sqrt{2} \text{Re}(u)}} + \\
& + \lambda^3 \omega^2 \frac{\sqrt{2} \text{Im}^2(u)}{[2 \text{Re}(u) (\text{Re}(u) + \sqrt{2}) + 2 \text{Im}^2(u) + 1]^{3/2}}
\end{aligned} \tag{4.2}$$

$$\tan(\theta_{23}) = 1 + 2\sqrt{2} \lambda \omega + \frac{\lambda^2}{2} [-1 + 4A - 2\sqrt{2} \text{Re}(u)] + \lambda^3 \omega (4\sqrt{2} A - 2 \text{Re}(u) + 12\sqrt{2} \omega^2 - \sqrt{2}) \tag{4.3}$$

$$\begin{aligned}
\tan(\theta_{12}) = & \tan(\tilde{\theta}_{12}) + \frac{\lambda \sigma (\sqrt{2}\tilde{c}_{12} + 2z)}{2\tilde{c}_{12}^3} + \frac{\lambda^2}{2\tilde{c}_{12}^3}\tilde{s}_{12} - \frac{\lambda^2\omega\sigma}{\tilde{c}_{12}^2} + \frac{\lambda^2 z\sqrt{2}\tilde{s}_{12}}{\tilde{c}_{12}^4} + \frac{3\lambda^2 z^2\tilde{s}_{12}}{2\tilde{c}_{12}^5} + \\
& + \frac{\lambda^3}{4\tilde{c}_{12}^4}\sigma \left[\sqrt{2}(1 - 2A\tilde{c}_{12}^2\rho) + \tilde{c}_{12}^2(\sqrt{2}|u|^2 + 2\text{Re}(u)) \right] + \\
& + \frac{\lambda^3}{2\tilde{c}_{12}^7} \left\{ -2\sqrt{2}\tilde{c}_{12}^4\omega(\tilde{c}_{12}\sigma\omega + \tilde{s}_{12}) + \tilde{c}_{12}^2z \left[\tilde{c}_{12}^2\sigma - 2\omega \sin(2\tilde{\theta}_{12}) + 3\sigma\tilde{s}_{12}^2 \right] + \right. \\
& \left. \frac{\tilde{c}_{12}\sigma z^2(5 - 3\cos(2\tilde{\theta}_{12}))}{\sqrt{2}} + \sigma z^3(3 - 2\cos(2\tilde{\theta}_{12})) \right\}
\end{aligned} \tag{4.4}$$

References

- [1] H. Minakata and A. Y. Smirnov, “Neutrino mixing and quark-lepton complementarity,” *Physical Review D* **70** no. 7, (Oct., 2004) .
<http://dx.doi.org/10.1103/PhysRevD.70.073009>.
- [2] H. Georgi and C. Jarlskog, “A New Lepton - Quark Mass Relation in a Unified Theory,” *Phys. Lett. B* **86** (1979) 297–300.
- [3] M. Raidal, “Relation between the neutrino and quark mixing angles and grand unification,” *Physical Review Letters* **93** no. 16, (Oct., 2004) .
<http://dx.doi.org/10.1103/PhysRevLett.93.161801>.
- [4] P. H. Frampton and R. N. Mohapatra, “Possible gauge theoretic origin for quark-lepton complementarity,” *Journal of High Energy Physics* **2005** no. 01, (Jan., 2005) 025–025.
<http://dx.doi.org/10.1088/1126-6708/2005/01/025>.
- [5] S. Antusch, S. King, and R. Mohapatra, “Quark–lepton complementarity in unified theories,” *Physics Letters B* **618** no. 1–4, (July, 2005) 150–161.
<http://dx.doi.org/10.1016/j.physletb.2005.05.026>.
- [6] Z.-Z. Xing, “Nontrivial correlation between the ckm and mns matrices,” *Physics Letters B* **618** no. 1–4, (July, 2005) 141–149.
<http://dx.doi.org/10.1016/j.physletb.2005.05.040>.
- [7] A. Datta, L. Everett, and P. Ramond, “Cabibbo haze in lepton mixing,” *Phys. Lett. B* **620** (2005) 42–51, [arXiv:hep-ph/0503222](https://arxiv.org/abs/hep-ph/0503222).
- [8] K. M. Patel, “An SO(10)XS4 Model of Quark-Lepton Complementarity,” *Phys. Lett. B* **695** (2011) 225–230, [arXiv:1008.5061](https://arxiv.org/abs/1008.5061) [hep-ph].
- [9] M. Picariello, B. C. Chauhan, J. Pulido, and E. Torrente-Lujan, “Predictions from non-trivial quark-lepton complementarity,” *International Journal of Modern Physics A* **22** no. 31, (Dec., 2007) 5860–5874. <http://dx.doi.org/10.1142/S0217751X07039080>.

- [10] B. Chauhan, M. Picariello, J. Pulido, and E. Torrente-Lujan, “Quark–lepton complementarity with lepton and quark mixing data predict $\theta_{13}^{PMNS} = (9_{-2}^{+1})^\circ$,” *The European Physical Journal C* **50** no. 3, (Feb., 2007) 573–578.
<http://dx.doi.org/10.1140/epjc/s10052-007-0212-z>.
- [11] J. Harada, “Neutrino mixing and cp violation from dirac-majorana bimaximal mixture and quark-lepton unification,” *Europhysics Letters (EPL)* **75** no. 2, (July, 2006) 248–253.
<http://dx.doi.org/10.1209/epl/i2006-10101-2>.
- [12] K. Zhukovsky and A. A. Davydova, “CP violation and quark-lepton complementarity of the neutrino mixing matrix,” *Eur. Phys. J. C* **79** no. 5, (2019) 385.
- [13] Y. Zhang, X. Zhang, and B.-Q. Ma, “Quark-lepton complementarity and self-complementarity in different schemes,” *Phys. Rev. D* **86** (2012) 093019, [arXiv:1211.3198 \[hep-ph\]](https://arxiv.org/abs/1211.3198).
- [14] X. Zhang, Y.-j. Zheng, and B.-Q. Ma, “Quark-lepton complementarity revisited,” *Phys. Rev. D* **85** (2012) 097301, [arXiv:1203.1563 \[hep-ph\]](https://arxiv.org/abs/1203.1563).
- [15] J. Barranco, F. Gonzalez Canales, and A. Mondragon, “Universal Mass Texture, CP violation and Quark-Lepton Complementarity,” *Phys. Rev. D* **82** (2010) 073010, [arXiv:1004.3781 \[hep-ph\]](https://arxiv.org/abs/1004.3781).
- [16] K. Cheung, S. K. Kang, C. S. Kim, and J. Lee, “Lepton flavor violation as a probe of quark-lepton unification,” *Physical Review D* **72** no. 3, (Aug., 2005) .
<http://dx.doi.org/10.1103/PhysRevD.72.036003>.
- [17] K. A. Hochmuth and W. Rodejohann, “Low and high energy phenomenology of quark-lepton complementarity scenarios,” *Physical Review D* **75** no. 7, (Apr., 2007) .
<http://dx.doi.org/10.1103/PhysRevD.75.073001>.
- [18] F. Plentinger, G. Seidl, and W. Winter, “The Seesaw mechanism in quark-lepton complementarity,” *Phys. Rev. D* **76** (2007) 113003, [arXiv:0707.2379 \[hep-ph\]](https://arxiv.org/abs/0707.2379).
- [19] S. K. Kang, “Revisiting the Quark-Lepton Complementarity and Triminimal Parametrization of Neutrino Mixing Matrix,” *Phys. Rev. D* **83** (2011) 097301, [arXiv:1104.1969 \[hep-ph\]](https://arxiv.org/abs/1104.1969).
- [20] H.-W. Ke, T. Liu, and X.-Q. Li, “Determination of the mixing between active neutrinos and sterile neutrino through the quark-lepton complementarity and self-complementarity,” *Phys. Rev. D* **90** no. 5, (2014) 053009, [arXiv:1408.1315 \[hep-ph\]](https://arxiv.org/abs/1408.1315).
- [21] J. Ferrandis and S. Pakvasa, “Quark-lepton complementarity relation and neutrino mass hierarchy,” *Phys. Rev. D* **71** (2005) 033004, [arXiv:hep-ph/0412038](https://arxiv.org/abs/hep-ph/0412038).

- [22] S. K. Kang, C. Kim, and J. Lee, “Importance of threshold corrections in quark–lepton complementarity,” *Physics Letters B* **619** no. 1–2, (July, 2005) 129–135.
<http://dx.doi.org/10.1016/j.physletb.2005.05.065>.
- [23] M. A. Schmidt and A. Y. Smirnov, “Quark Lepton Complementarity and Renormalization Group Effects,” *Phys. Rev. D* **74** (2006) 113003,
[arXiv:hep-ph/0607232](https://arxiv.org/abs/hep-ph/0607232).
- [24] A. Dighe, S. Goswami, and P. Roy, “Quark-lepton complementarity with quasidegenerate majorana neutrinos,” *Physical Review D* **73** no. 7, (Apr., 2006) .
<http://dx.doi.org/10.1103/PhysRevD.73.071301>.
- [25] J. Ferrandis and S. Pakvasa, “A Prediction for $—U(e3)—$ from patterns in the charged lepton spectra,” *Phys. Lett. B* **603** (2004) 184–188, [arXiv:hep-ph/0409204](https://arxiv.org/abs/hep-ph/0409204).
- [26] D. Meloni, “Bimaximal mixing and large θ_{13} in a SUSY SU(5) model based on S_4 ,” *JHEP* **10** (2011) 010, [arXiv:1107.0221](https://arxiv.org/abs/1107.0221) [hep-ph].
- [27] J. Harada, “Non-maximal θ_{23} , large θ_{13} and tri-bimaximal θ_{12} via quark-lepton complementarity at next-to-leading order,” *EPL* **103** no. 2, (2013) 21001,
[arXiv:1304.4526](https://arxiv.org/abs/1304.4526) [hep-ph].
- [28] G. Sharma and B. C. Chauhan, “Quark-lepton complementarity predictions for θ_{23}^{pmns} and CP violation,” *JHEP* **07** (2016) 075, [arXiv:1511.02143](https://arxiv.org/abs/1511.02143) [hep-ph].
- [29] P. F. Harrison, D. H. Perkins, and W. G. Scott, “Tri-bimaximal mixing and the neutrino oscillation data,” *Phys. Lett. B* **530** (2002) 167, [arXiv:hep-ph/0202074](https://arxiv.org/abs/hep-ph/0202074).
- [30] F. Feruglio and A. Paris, “The golden ratio prediction for the solar angle from a natural model with a 5 flavour symmetry,” *Journal of High Energy Physics* **2011** no. 3, (Mar., 2011) . [http://dx.doi.org/10.1007/JHEP03\(2011\)101](http://dx.doi.org/10.1007/JHEP03(2011)101).
- [31] C. Jarlskog, “Commutator of the quark mass matrices in the standard electroweak model and a measure of maximal CP nonconservation,” *Phys. Rev. Lett.* **55** (Sep, 1985) 1039–1042. <https://link.aps.org/doi/10.1103/PhysRevLett.55.1039>.
- [32] “Unitary triangle fit,” <http://www.utfit.org/UTfit/ResultsSummer2023SM>.
- [33] I. Esteban, M. C. Gonzalez-Garcia, M. Maltoni, T. Schwetz, and A. Zhou, “The fate of hints: updated global analysis of three-flavor neutrino oscillations,” *JHEP* **09** (2020) 178,
[arXiv:2007.14792](https://arxiv.org/abs/2007.14792) [hep-ph].
- [34] “Nufit 5.3 (2024),” <http://www.nu-fit.org/>.
- [35] **Super-Kamiokande** Collaboration, K. Abe *et al.*, “Atmospheric neutrino oscillation analysis with external constraints in Super-Kamiokande I-IV,” *Phys. Rev. D* **97** no. 7, (2018) 072001, [arXiv:1710.09126](https://arxiv.org/abs/1710.09126) [hep-ex].

- [36] Y. Farzan and A. Y. Smirnov, “Leptonic CP violation: Zero, maximal or between the two extremes,” *JHEP* **01** (2007) 059, [arXiv:hep-ph/0610337](#).
- [37] G. Altarelli and F. Feruglio, “Models of neutrino masses and mixings,” *New J. Phys.* **6** (2004) 106, [arXiv:hep-ph/0405048](#).
- [38] P. F. de Salas, D. V. Forero, S. Gariazzo, P. Martínez-Miravé, O. Mena, C. A. Ternes, M. Tórtola, and J. W. F. Valle, “2020 global reassessment of the neutrino oscillation picture,” *JHEP* **02** (2021) 071, [arXiv:2006.11237 \[hep-ph\]](#).
- [39] F. Capozzi, E. Di Valentino, E. Lisi, A. Marrone, A. Melchiorri, and A. Palazzo, “Unfinished fabric of the three neutrino paradigm,” *Phys. Rev. D* **104** no. 8, (2021) 083031, [arXiv:2107.00532 \[hep-ph\]](#).
- [40] F. Feroz and M. P. Hobson, “Multimodal nested sampling: an efficient and robust alternative to MCMC methods for astronomical data analysis,” *Mon. Not. Roy. Astron. Soc.* **384** (2008) 449, [arXiv:0704.3704 \[astro-ph\]](#).
- [41] F. Feroz, M. P. Hobson, and M. Bridges, “MultiNest: an efficient and robust Bayesian inference tool for cosmology and particle physics,” *Mon. Not. Roy. Astron. Soc.* **398** (2009) 1601–1614, [arXiv:0809.3437 \[astro-ph\]](#).
- [42] F. Feroz, M. P. Hobson, E. Cameron, and A. N. Pettitt, “Importance Nested Sampling and the MultiNest Algorithm,” *Open J. Astrophys.* **2** no. 1, (2019) 10, [arXiv:1306.2144 \[astro-ph.IM\]](#).